

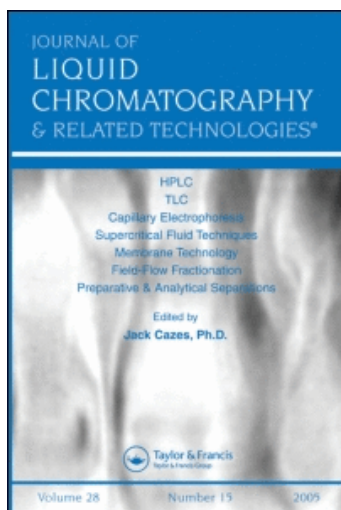
This article was downloaded by: [CAS Chinese Academy of Sciences]

On: 25 September 2010

Access details: Access Details: [subscription number 906718089]

Publisher Taylor & Francis

Informa Ltd Registered in England and Wales Registered Number: 1072954 Registered office: Mortimer House, 37-41 Mortimer Street, London W1T 3JH, UK



## Journal of Liquid Chromatography & Related Technologies

Publication details, including instructions for authors and subscription information:

<http://www.informaworld.com/smpp/title~content=t713597273>

### Investigation of Electroosmotic Flow in Nanosilica Particle Packed Capillaries

Yangjun Ding<sup>a</sup>; Jiping Ma<sup>b</sup>; Lingxin Chen<sup>c</sup>

<sup>a</sup> Department of Chemical Engineering, Qufu Normal University, Qufu, P.R. China <sup>b</sup> Institute of Environment & Municipal Engineering, Qingdao Technological University, Qingdao, P.R. China <sup>c</sup> Yantai Institute of Coastal Zone Research for Sustainable Development, Chinese Academy of Sciences, Yantai, P.R. China

**To cite this Article** Ding, Yangjun , Ma, Jiping and Chen, Lingxin(2008) 'Investigation of Electroosmotic Flow in Nanosilica Particle Packed Capillaries', Journal of Liquid Chromatography & Related Technologies, 31: 17, 2541 — 2553

**To link to this Article:** DOI: 10.1080/10826070802352710

**URL:** <http://dx.doi.org/10.1080/10826070802352710>

PLEASE SCROLL DOWN FOR ARTICLE

Full terms and conditions of use: <http://www.informaworld.com/terms-and-conditions-of-access.pdf>

This article may be used for research, teaching and private study purposes. Any substantial or systematic reproduction, re-distribution, re-selling, loan or sub-licensing, systematic supply or distribution in any form to anyone is expressly forbidden.

The publisher does not give any warranty express or implied or make any representation that the contents will be complete or accurate or up to date. The accuracy of any instructions, formulae and drug doses should be independently verified with primary sources. The publisher shall not be liable for any loss, actions, claims, proceedings, demand or costs or damages whatsoever or howsoever caused arising directly or indirectly in connection with or arising out of the use of this material.



## Investigation of Electroosmotic Flow in Nanosilica Particle Packed Capillaries

Yangjun Ding,<sup>1</sup> Jiping Ma,<sup>2</sup> and Lingxin Chen<sup>3</sup>

<sup>1</sup>Department of Chemical Engineering, Qufu Normal University, Qufu, P.R. China

<sup>2</sup>Institute of Environment & Municipal Engineering, Qingdao Technological University, Qingdao, P.R. China

<sup>3</sup>Yantai Institute of Coastal Zone Research for Sustainable Development, Chinese Academy of Sciences, Yantai, P.R. China

**Abstract:** An experimental investigation of electroosmotic flow (EOF) in nanosilica particle packed capillaries was carried out. The packed capillaries were fabricated by packing 10 nm, 30 nm, 50 nm, and 360 nm nanosized silica particles into fused silica capillaries of 5 cm × 320 μm i.d. × 800 μm o.d. The EOF within the packed capillary was characterized and evaluated by measuring the EOF, as well as the electric properties using two salt free liquids: water, methanol, and an aqueous 1–1 electrolyte liquid: sodium chloride solution. The results reflected the influence of the electric double layer (EDL) on the EOF in nanochannel interspaces, which would be helpful for nanochannel study in microfluidic and nanofluidic systems and capillary electroseparation (CES) methods that involve chromatography stationary phase research.

**Keywords:** Capillary electroseparation (CES), Electroosmotic Flow (EOF), Interspace, Microfluidic, Nanochannel, Nanofluidic

Correspondence: Dr. Lingxin Chen, Yantai Institute of Coastal Zone Research for Sustainable Development, Chinese Academy of Sciences, 264003, Yantai, China. E-mail: chenlx@mail.tsinghua.edu.cn; majiping2001@yahoo.com.cn



## INTRODUCTION

Further downsizing the microfluidic channels to the nanoscale is attractive for both fundamental studies, such as fluid transport and molecular behavior at extremely small dimensions<sup>[1,2]</sup> and in technical applications such as manipulation and high sensitivity detection of single molecules for biosensing, chemical analysis, and medical diagnostics.<sup>[3,4]</sup> The study and usage of nanochannels are more recently appearing<sup>[5,6]</sup> Kuo et al.<sup>[7]</sup> have investigated molecular transport through nanoporous nuclear track etched (PCTE) membranes with 15–200 nm diameter cylindrical pores using fluorescent probes, by manipulating applied electric field polarity, pore size, membrane surface functionality, pH, and the ionic strength. And they have<sup>[8,9]</sup> used commercially available 6–10  $\mu\text{m}$  thick nanoporous PCTE membranes containing nanometer diameter capillaries as gateable interconnects, to form a 3-dimensional hybrid microfluidic and nanofluidic system in polydimethylsiloxane (PDMS) chips. Karlsson et al.<sup>[10]</sup> have presented fluidic control in lipid nanotubes 50–150 nm in radius, conjugated with surface immobilized unilamellar lipid bilayer vesicles (5–25  $\mu\text{m}$  in diameter). Conlisk et al.<sup>[11]</sup> have examined the fluid flow and mass transfer under an electric field in a rectangular microchannel and nanochannel. In fact, as early as middle 1960s, Burgreen et al.<sup>[12]</sup> had already reported a similar study of electrokinetic flow (EKF) in very fine capillary channels of rectangular cross section, just like those channels in chips nowadays, which was a natural extension of the general theory of EKF.

The fundamental challenges imposed on fabricating low cost nanofluidic channels are to define nanoscale trenches or matrices and to seal these templates to complete functional nanofluidic devices. Typical methods of fabricating nanofluidic channels include using electron beam lithography and focused ion beam milling techniques to fabricate high resolution nanoscale templates, combined with wafer bonding; channel formation by using sacrificial materials; or channel sealing by using PDMS polymers.<sup>[13]</sup> Guo et al.<sup>[14]</sup> have presented an approach to fabricate nanofluidic channels with well controlled dimensions by imprinting a channel template into a thin polymer film cast on a glass cover slip in a singlestep. To investigate the nanochannels characteristics related to the nanofluidic chips such as EKF, are more difficult because the key feature of a nanofluidic channel is that fluid flow occurs in structures of the same size as the physical parameters that govern the flow.<sup>[15,16]</sup> Rice et al.<sup>[15]</sup> have presented a theoretical study of EKF in narrow cylindrical capillaries, which was concerned with the dependence of usual electrokinetic phenomena on the electrokinetic radius. The radius obtained for this dependence must, however, be treated with caution for the higher values of the interface potential due to the use of the Debye-Huckel



approximation. Control of fluid delivery inside small dimension channels is of paramount importance in microfluidic devices. When using smaller channel dimensions (low nanoscale), it becomes difficult not only to fabricate the channels using traditional microfabrication techniques but also to handle and manipulate the flow of fluid inside the channels. For these decreasing scales, where channel dimensions are approaching the size of a single large protein, fluidic devices capable of handling single molecules might be realized. The EOF in a single nanochannel is difficult to measure at present. To achieve this, new materials, new principles of fluid delivery, and new fabrication techniques might be necessary to develop.

Liquid chromatography has seen a dramatic increase in speed and efficiency over the past decade. The advances in separation speed have been mostly related to the development of column technology and instrumentation. The column technology includes small uniform particles, monolithic columns, and thermally stable phases with various bonding chemistries. In recent years, we have noticed that improvements in chromatographic efficiency and analysis time have been demonstrated by the use of small stationary phase support particles (sub-2  $\mu\text{m}$  particles) packed into relatively long (>20 cm) fused silica capillary columns. This technique has been termed ultrahigh pressure liquid chromatography (UPLC) because of the extreme pressures required to force mobile phase through these columns (>1400 bar, or 20 000 psi). To date, UPLC has been performed using 670 nm organosilica nano particles,<sup>[17]</sup> 1.0  $\mu\text{m}$  non-porous silica particles,<sup>[18]</sup> and 1.5  $\mu\text{m}$  porous ethyl-bridged hybrid particles<sup>[19]</sup> as the stationary phase support material. Capillary electroseparation (CES) methods such as capillary electrochromatography (CEC), involve the application of high voltages across the lengths of the small bore tubes packed with fine particles. To date, the particles diameters ranging from minimum 500 nm to about normally 1  $\mu\text{m}$ , 3  $\mu\text{m}$ , and 5  $\mu\text{m}$  are often used by various CES methods. The diameters limits of stationary phase support particles for CES methods are restricted to the EDL overlap. The experimental investigation of electroosmotic flow (EOF) in nanosilica particle packed capillaries would be obviously helpful for better use of the CES methods.

In this work, based on the previous work on electroosmotic pump (EOP) research,<sup>[20–24]</sup> the packed capillaries with nanochannels were fabricated by packing the 10 nm, 30 nm, 50 nm, and 360 nm silica particles into short fused silica capillaries. Although our method provides us statistical results of the characteristics of equivalent nanochannels, they are valuable in giving some hints on nanochannel study on microfluidic and nanofluidic chip systems or helpful in electrical separation methods that involve chromatography stationary phases research.



## EXPERIMENTAL

The monodisperse uniform nanosized silica particles were prepared by the method of Stöber et al.<sup>[25]</sup> Generally, hydrolysis is a very slow reaction, though acids or bases are used as catalysts. Ammonium hydroxide has been used as a catalyst for improving hydrolysis and condensation of tetraethyl orthosilicate (TEOS) in ethanol.<sup>[26]</sup> As shown in Table 1, four different dispersions of nanosilica particles (designated as A, B, C, and D) could be prepared by hydrolysis of TEOS in ethanol medium in the presence of ammonium hydroxide. TEOS, absolute ethanol used as the solvent, and 28% ammonium hydroxide were reagent grade. Glassware was cleaned with 10% hydrogen chloride and rinsed with distilled water and absolute ethanol. A total of 1 mL of TEOS were added to 25 mL of ethanol within screw cap vials, in the presence of different amounts of  $\text{NH}_4\text{OH}$  (0.92, 1.14, 1.5, and 7 mL, respectively, in samples A, B, C, and D) and placed overnight. Then, we can obtain four different sizes of silica nanoparticles, i.e., 30 nm, 50 nm, 100 nm, and 360 nm. We used a gravitational sedimentation method to screen the smallest sized particles, 10 nm, from the 30 nm nanosilica particles slurry, by drawing the slurry solutions positioned at a relatively top depth (5 cm deep). Figure 1 was the transmission electron microscope (TEM) photographs of 30 nm, 50 nm, 100 nm, and 360 nm particles, some of which will be used in the following experiments. There was unsaturated incomplete bonds and oxhydryl in different linkage in the surface of nanosilica particles, as its surface was oxygen debt, it deviated from stable silicon oxygen structure, so formulate was often written as  $\text{SiO}_{2-x}$  ( $x = 0.4 \sim 0.8$ ).

The nanosilica particle packed columns were fabricated using the slurry packed method assisted with a high power supply.<sup>[20–24,27–29]</sup> Briefly, the packed capillary was fabricated with three steps. First, the frit at one end of the capillary was fabricated using a sodium silicate paste mixed with  $2\text{ }\mu\text{m}$  porous silica particles (Dalian Institute of Chemical Physics, Chinese Academic of Sciences, China) and heated in an automatic time programmed oven about  $300^\circ\text{C}$  for about 10–20 seconds, then a nanosilica particle slurry was pumped into the capillary and the filter

**Table 1.** Conditions for different dispersions of nanosilica particles

	EtOH/mL	$\text{NH}_4\text{OH}$ /mL	TEOS/mL	Size/nm
A	25	0.92	1	$20 < d < 30$
B	25	1.14	1	$70 < d < 80$
C	25	1.5	1	$100 < d < 120$
D	25	7.0	1	$340 < d < 350$



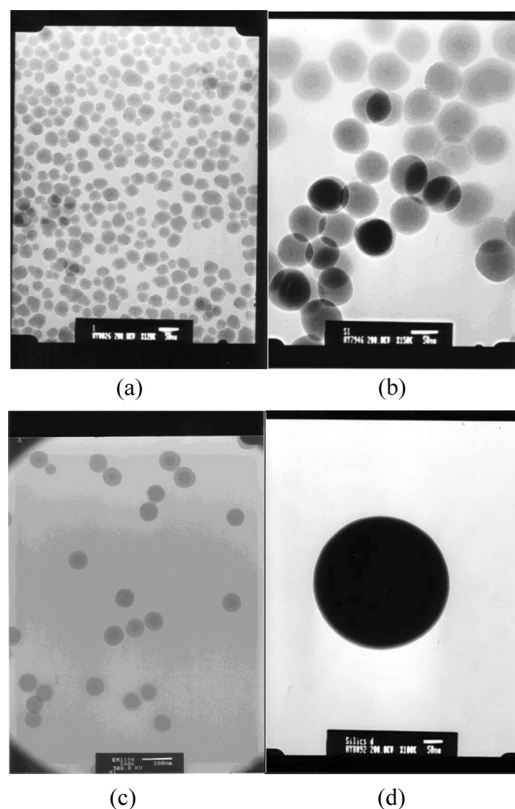


**Figure 1.** TEM micrographs of nanosilica particles, (a) 30 nm, (b) 50 nm, (c) 100 nm, and (d) 360 nm. The scale bars of (a), (b), (c), and (d) are 50 nm, 50 nm, 200 nm, and 50 nm, respectively.

like “frit” retained the nanosilica particles in place and then the second frit was formed by heating the other end of the packed capillary with the sodium silicate paste. The packed capillary was equilibrated with methanol for an hour at high electric field and conditioned with pure water for another two hours before use. In the nanoparticle packed capillary, the interstitial spaces between the particles act like multiple flow passages with the nanochannel in parallel. In order to measure the actual EOF of the packed capillary, we designed a system as shown in Figure 2. A micro volume injector with volume of  $5\ \mu\text{L}$  and a stopwatch was used to measure the volumetric flow rate. Each measurement was carried out 6 times when the EOF of the column was conditioned and stable for 2 h using the liquid delivered. Methanol and acetonitrile were chromatographic grade. Sodium chloride was AR grade. The water was purified with Milli-Q.



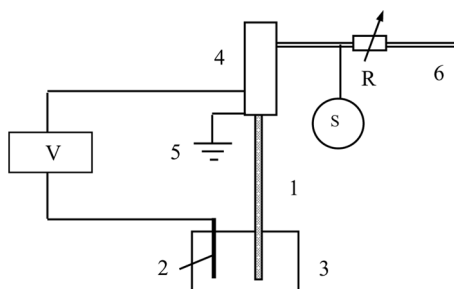


**Figure 2.** Schematic diagram of the system used for EOF measurements: (V) a high power supply with an amperometer, (1) a nanosilica packed capillary, (2) a positive pole and a Pt wire, (3) sodium chloride electrolyte solution or water, (4) a two-channel electrode and the negative pole (ground electrode 5), (R) regulating flow resistance, (S) pressure sensor, and (6) output channel, through which the EOF was monitored.

## RESULTS AND DISCUSSION

Over the past two decades there has been intense interest in CES methods, such as capillary zone electrophoresis (CZE) and CEC, which involve the application of high voltages across the lengths of the small bore tubes or the capillary column packed with fine particles. Migration of solutes within a CES system arises from one or both of the following phenomena: electrophoresis and electroosmosis, namely electrokinetic flow (EKF). In this work, the electroosmosis would be the dominating factor in low ionic strength solutions ( $\sim 10$  mM) because the liquids used in our experiments are salt free liquids; pure water, methanol, or an entirely dissociated sodium chloride solution with a maximum concentration of  $7 \times 10^{-3} \text{ mol/L}^{-1}$ .<sup>[7]</sup> Surfaces, such as glass or quartz, nearly always possess charged groups, which are permanently attached to the surface, for example,  $-\text{SiO}^-$  groups in the case of silica bear fixed negative charges, while the solution in contact with them contains an equivalent excess of positively charged ions, forming an electrical double layer (EDL), the immovable inner Helmholtz plane (IHP) and movable outer Helmholtz plane (OHP). The OHP forms a net positive region of ions that span a distance on the order of the Debye length. The EOF arises from a balance between the electrical forces on the excess ions on the solution side of the double layer, and the viscous drag of the liquid in the layer. In a fine silica packed capillary, the interstitial spaces between the particles act like multiple flow passages with very small diameter in parallel. The total behavior of EOF in the packed channel can be estimated by using the behavior of EOF in a single capillary. The net electroosmotic flow rate,  $Q$ , of a liquid in the capillary, is linearly superposed of



the electroosmotic flow with the counter flow.<sup>[15]</sup> The total flow rate of the entire porous medium is then

$$Q = -\frac{pA\varepsilon_r\varepsilon_0\zeta V}{\tau^2\eta L}\left(1 - \frac{2I_1(\kappa a)}{\kappa aI_0(\kappa a)}\right) - \frac{pA\Delta Pa^2}{8\tau^2\eta L} \quad (1)$$

where the minus sign in the first term of Equation 1 means that when the zeta potential,  $\zeta$ , is negative, the direction of electroosmotic velocity is the same as that of electric field intensity  $E$ ;  $p$  is porosity of the packed capillary ( $p = V_{\text{dry}}/V_{\text{wet}}$ , where  $V_{\text{dry}}$  and  $V_{\text{wet}}$  are the void and total volumes of the packing materials, respectively);  $\tau$  is the tortuosity of the packed capillary ( $\tau = L_e/L$ , where  $L_e$  is the average length of migration along the pore path and  $L$  the physical length of the packed channel);  $A$  is the cross sectional area of the packed channel;  $\varepsilon$  is the dielectric constant,  $\zeta$  is the zeta potential of the packing materials;  $E$  is the electric intensity;  $\eta$  is the viscosity of the liquid;  $\kappa$  is the reciprocal of the double layer thickness;  $a$  is the average pore radius of particles;  $\Delta P$  is the pressure difference along the length of the capillary (negative minus positive); and  $I_0$ ,  $I_1$  are the zero order and first order modified Bessel function of the first kind, respectively. Equation 1 applies when the thickness of the double layer  $\kappa^{-1}$  is much less than the extent of the electrolyte beyond the double layer. The distance over which the excess charge concentration falls off by the factor  $e(2.718)$  is called the 'double layer thickness'. The double layer thickness,  $\kappa^{-1}$ , is given by

$$\kappa^{-1} = \left(\frac{\varepsilon_0\varepsilon_r RT}{2cF}\right)^{1/2} \quad (2)$$

where  $R$  is universal gas constant,  $T$  is absolute temperature,  $c$  is molar concentration medium,  $F$  is Faraday constant. For  $c = 1 \times 10^{-3} \text{ mol/L}^{-1}$  and  $100 \times 10^{-3} \text{ mol/L}^{-1}$  aqueous 1-1 electrolyte  $\kappa^{-1} = 10 \text{ nm}$  and  $1 \text{ nm}$ , respectively. If the internal diameter of an open capillary,  $d$ , is larger than about 10 times the double layer thickness,  $\kappa^{-1}$ , the double layer overlap will have no obvious influence and the mean velocity not be affected. Similarly, for a packed capillary the overall EOF is independent of the particle diameter, at least down to a size at which the mean interspace channel diameter,  $d_c$ , in the packed bed becomes comparable to the double layer thickness,  $\kappa^{-1}$ , of at least  $10 \kappa^{-1}$ . As has been shown by Knox et al.<sup>[30-32]</sup> on the basis of the previous work of Rice et al.,<sup>[15]</sup> since the channels in beds of spheres are approximately 1/4-1/5 of the mean sphere diameter, the EOF rate is expected to remain unchanged until the particle diameter in the packed bed falls to below about  $40 \kappa^{-1}$ . For aqueous electrolyte solutions having ionic strengths of  $1 \times 10^{-3} \text{ mol/L}^{-1}$ ,  $10 \times 10^{-1} \text{ mol/L}^{-1}$  and  $100 \times 10^{-3} \text{ mol/L}^{-1}$ , the double layer thickness,  $\kappa^{-1}$ , is 10 nm, 3 nm, and 1 nm, and the minimum particle diameters  $d_p$  will then be 0.4, 0.12, and 0.04  $\mu\text{m}$ , respectively. The general validity of this was



confirmed by Knox et al., who demonstrated that there is indeed no significant loss of electroosmotic velocity with particles down to 1.5 or even 0.5  $\mu\text{m}$  in diameter.<sup>[32]</sup> The nanosilica particles with particle diameter,  $d_p$ , of 10 nm, 30 nm, 50 nm, and 360 nm could be used to experimentally investigate the particle diameter limit related to the EOF in a packed capillary. Based on the facts analyzed above, all the packed capillaries made cannot be used to generate the EOF, except for the 360 nm silica capillary, even at  $100 \times 10^{-3} \text{ mol/L}^{-1}$  aqueous electrolyte solutions. What really is the particle diameter limit for generating the EOF in packed capillaries?

When a current is passed along the nanosilica packed capillary, a cylindrical conductor, ohmic heat is released and the capillary heats up. This is a common problem for any electrical driven technique. The heat so generated is conducted from the central region of the packed capillary, first through the walls of the capillary and then surrounding the air. Investigating the real time EOF of the nanosilica capillary, the ohmic heat should be conducted immediately and controlled as little as possible. In order to simplify the experiments, we have carried out the experiments at air surrounding about  $10^\circ\text{C}$  and measured current voltage relationship, of the ohm curve of the packed capillary. Figure 3 is the electrical current vs. driven

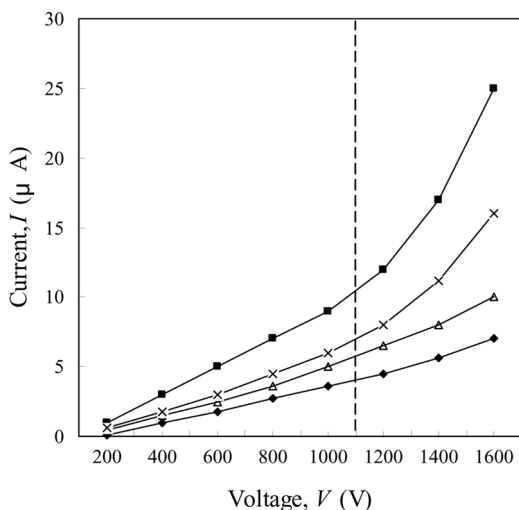


**Figure 3.** Electrical current vs. driven voltage or electric field ( $V/5 \text{ cm}$ ), Ohm curve of the packed capillary. ◆, 50 nm nanosilica particle and  $3.0 \times 10^{-3} \text{ mol/L}$  NaCl, Δ, 50 nm nanosilica particle and  $7.0 \times 10^{-3} \text{ mol/L}$  NaCl, ×, 360 nm nanosilica particle and  $3.0 \times 10^{-3} \text{ mol/L}$  NaCl, ■, 360 nm nanosilica particle and  $7.0 \times 10^{-3} \text{ mol/L}$  NaCl. (From the bottom). The current-voltage relationship of the packed capillary was good linearity when the driven voltage was less than 1000 V (left of the dashed-line).



voltage or electric field, using 50 nm nanosilica and 360 nm nanosilica particles. We can find that the current voltage relationship of the packed capillary had good linearity when the driven voltage was less than 1000 V (i.e.,  $E$  200 V  $\cdot$  cm $^{-1}$ ), and  $R^2$  of the trendline linear equation was 0.99. Therefore, the driven voltages were controlled below 1000 V, the EOF in the interspaces of the nanosilica packed capillary is generated with high efficiency, and the bubble formation could be ignored; and in this way the EOF measured could reflect the influence of the EDL on the EOF in nanochannel interspaces of packed capillary. Moreover, the electrical current of a 50 nm nanosilica packed capillary was less than that of 360 nm nanosilica packed capillary, due to it relatively less porosity and more electrical resistance.

In the micro size silica particles packed capillary, the same principles as a narrow open capillary apply, but there are now numerous interconnected flow channels, which are no longer uniform in size, shape, or direction. Nevertheless, a given silica material will exhibit the same zeta potential whether it is in the form of particles or an open capillary.<sup>[32]</sup> A given nanosilica packed capillary will exhibit the similar zeta potential, but the EOF will be much lower. The most important is the difference between normal particles used previously and nanosilica particles used in our work. The normal particles mean that the particles diameter is from 500 nm to about 5  $\mu$ m (often used by various packed bed EOPs and CES methods nowadays), the channel interspaces equivalent diameters will be about from 100 nm to about 1.00  $\mu$ m when packed in a capillary. The EDL overlap will not occur at this circumstance based on the work of Knox et al.<sup>[30–32]</sup> Because of the double layer thickness,  $\kappa^{-1}$ , which characterizes the length scale of ionic interactions in aqueous electrolyte solutions, spans the range 3 nm <  $\kappa^{-1}$  < 10 nm when the ionic strength,  $I$ , of the buffer solution lies in 1–10 mmol/L range. In this paper, when the nanosilica particles with particles diameters of 10 nm, 30 nm, 50 nm, and 360 nm are used, the channel interspaces equivalent diameters will be about from 2 nm, 6 nm, and 10 nm to 72 nm. Obviously, the EDL overlap will occur seriously even at a higher ionic strength, for example, 10 mmol/L, and it seems that it is impossible for such small particles used to generate EOF. Figure 4 shows the actual relationship between maximum flow rates  $Q$  ( $\mu$ L min $^{-1}$ ) and applied voltage  $V$  (V) using pure water, methanol, and sodium chloride solution, using 50 nm and 360 nm nanosilica particles. The flow rate for every liquid being delivered increased linearly with the increase of applied voltage. The flow rate values sequence was:  $3 \times 10^{-3}$  mol/L NaCl solution (360 nm silica)  $\approx$  pure water (50 nm silica) >  $0.5 \times 10^{-3}$  mol/L NaCl solution (360 nm silica) >  $0.5 \times 10^{-3}$  mol/L NaCl solution (50 nm silica) > methanol (50 nm silica).

For 360 nm silica columns, it was easy to understand that the flow rate values increased with the increase of the concentration of the



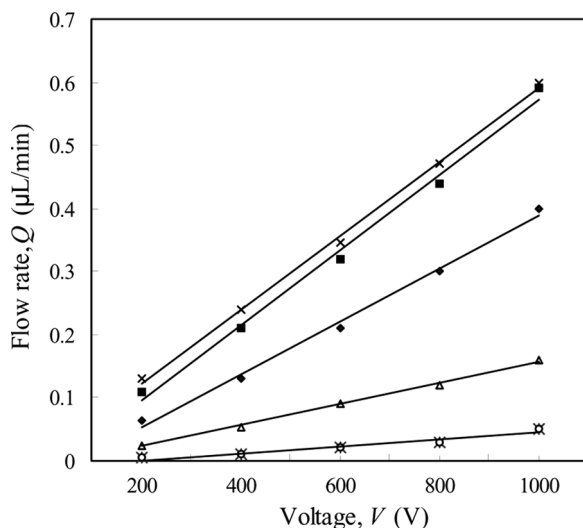


**Figure 4.** Maximum electroosmotic flow rate  $Q$  ( $\mu\text{L}/\text{min}$ ) vs. driven voltage  $V$  (V). □, 50 nm nanosilica particle and methanol, Δ, 50 nm nanosilica particle and  $0.5 \times 10^{-3}$  mol/L NaCl, ◆, 360 nm nanosilica particle and  $0.5 \times 10^{-3}$  mol/L NaCl, ■, 360 nm nanosilica particle and  $3.0 \times 10^{-3}$  mol/L NaCl, × 50 nm nanosilica particle and water. (From the bottom).

NaCl solution,  $3 \times 10^{-3}$  mol/L NaCl solution (360 nm silica)  $>$   $0.5 \times 10^{-3}$  mol/L NaCl solution (360 nm silica). For 50 nm silica columns, the expected values of the flow rates sequence was  $0.5 \times 10^{-3}$  mol/L NaCl solution (50 nm silica)  $>$  pure water (50 nm silica)  $>$  methanol (50 nm silica) because of the ionic and/or polarity sequence of the liquids being delivered. The actual result was: pure water (50 nm silica)  $>$   $0.5 \times 10^{-3}$  mol/L NaCl solution (50 nm silica)  $>$  methanol (50 nm silica). These results revealed that the  $0.5 \times 10^{-3}$  mol/L NaCl solution was enough to restrict the EDL and significant loss of EOF, making the EOF value of the pure water much more than that of  $0.5 \times 10^{-3}$  mol/L NaCl solution. For a 1–1 sodium chloride electrolyte, EDL,  $\kappa^{-1}$ , according to the Stern-Gouy-Chapman theory is given by Equation 2. For a concentration of  $c = 0.5 \times 10^{-3}$  mol/L NaCl solution, with water as solvent (for which the relative dielectric constant is  $\epsilon_r = 80$ ), Equation 2 gives the thickness of the double layer,  $\kappa^{-1}$ , as 14 nm. When  $d_c$  approaches  $\kappa^{-1}$ , double layer overlap occurs and eventually when  $d$  is of the same order as  $\kappa^{-1}$ , the flow velocity is much reduced and the velocity profile approaches parabolic, which was analyzed in detail by Rice et al.<sup>[15]</sup> This calculation is suitable for the 360 nm silica packed capillary, but the EOF is impossible in the 50 nm silica packed capillary because the mean interspace channel diameter,  $d_c$ , in the packed bed is only about 10 nm and is less than the



double layer thickness. From Figure 4, we find that for a concentration of  $c = 0.5 \times 10^{-3}$  mol/L NaCl solutions, the flow rate of the 50 nm silica particle packed capillary is about one third of the 360 nm silica particle, which shows that the double layer overlap is not as significant as expected. The unusual physical and chemical characteristics of nanosilica could account for this. There are unsaturated incomplete bonds and oxhydryl in a different linkage in the nanosilica surface, as its surface is oxygen debt. It deviates from stable silicon oxygen structure, the percent of surface oxhydryl of 50 nm nanosilica used is estimated about 30% of stable silicon oxygen structure, for example, and the zeta potential as well as the thickness of the double layer,  $\kappa^{-1}$ , is about one third of that supposed as a rule of thumb.

An important consideration is the dependence of zeta potential,  $\zeta$ , upon electrolyte concentration, since  $Q$  is directly proportional to  $\zeta$ . There is no doubt that  $\zeta$  decreases with electrolyte concentration. The effect of sodium chloride concentrations on the EOF of the packed capillary is shown in Figure 5, which was the result of maximum flow rate vs. applied voltage with the sodium chloride with the different concentrations. For the 360 nm silica packed capillary, the electrolyte

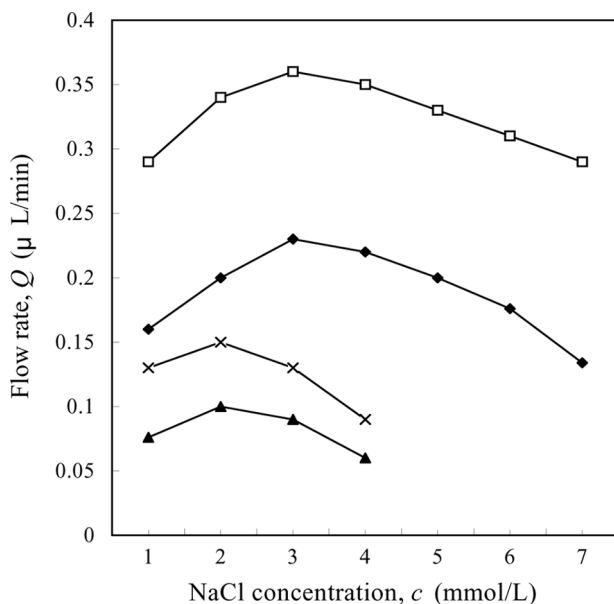


**Figure 5.** Effect of sodium chloride concentration,  $c$  ( $\times 10^{-3}$  mol/L), on electroosmotic flowrate  $Q$  ( $\mu\text{L}/\text{min}$ ), at various applied voltage  $V$  (V).  $\blacktriangle$ , 50 nm nanosized silica particle and 400 V,  $\times$ , 50 nm nanosized silica particle and 600 V,  $\blacklozenge$ , 360 nm nanosized silica particle and 400 V,  $\square$ , 360 nm nanosized silica particle and 600 V. (From the bottom).



concentration has some effects on the EOF at the range from  $0.5 \times 10^{-3}$  mol/L to  $7 \times 10^{-3}$  mol/L. When sodium chloride concentrations were less than  $3 \times 10^{-3}$  mol/L, the flow rates of the capillary were all significantly proportional to sodium chloride concentrations with different driven voltages. When sodium chloride concentrations were more than  $3 \times 10^{-3}$  mol/L, the flow rates of the capillary decreased with the concentrations of sodium chloride solution. There was a similar relationship for the 50 nm silica packed capillary only with the concentration range of sodium chloride solution decreased at about  $2 \times 10^{-3}$  mol/L. Because the Joule heating was very small, the EDL, as well as the thermodynamic efficiency, accounts for the difference between them.

## CONCLUSIONS

The nanosilica particles with particle diameter,  $d_p$ , of 10 nm, 30 nm, 50 nm, and 360 nm were used to investigate the EOF in nanosilica particle packed capillaries. The EOF within the packed capillary was characterized and evaluated by measuring the EOF, as well as the electric properties using two salt free liquids: water, methanol, and an aqueous 1–1 electrolyte liquid: sodium chloride solution. We have found that EOF decreased more or less linearly towards zero as  $d_p$  fell from 50 nm, 30 nm, to 10 nm for any electrolyte solutions from which the equivalent nanochannel interspaces diameters about 10 nm to 2 nm were fabricated. For a 10 nm silica particle capillary we could hardly measure the EOF using  $1 \times 10^{-5}$  mol/L sodium chloride solution. The results reported in this paper reflected the influence of the EDL on the EOF in nanochannel interspaces, which would be helpful for nanochannel study in microfluidic and nanofluidic systems and CES methods that involve widely used nanosilica based chromatography stationary phases research.

## ACKNOWLEDGMENT

The authors acknowledge the support from the Education Commission Natural Science Foundation of Shandong Province (J07WZ05) and the Qingdao Technological University Research Startup Grant (c2007-008).

## REFERENCES

1. Turner, S.W.P.; Cabodi, M.; Craighead, H.G. *Phys. Rev. Lett.* **2002**, *88*, 128103.
2. Bakajin, O.B.; Duke, T.A.J.; Chou, C.-F.; Chan, S.S.; Austin, R.H.; Cox, E.C. *Phys. Rev. Lett.* **1998**, *80*, 2737.



3. Levene, M.J.; Korlach, J.; Turner, S.W.; Foquet, M.; Craighead, H.G.; Webb, W.W. *Science* **2003**, *299*, 682.
4. Tegenfeldt, J.O.; Bakajin, O.; Chou, C.-F.; Chan, S.; Austin, R.H.; Chan, E.; Duke, T.; Cox, E.C. *Phys. Rev. Lett.* **2001**, *86*, 1378.
5. Foquet, M.; Korlach, J.; Zipfel, W.; Webb, W.W.; Craighead, H.G. *Anal. Chem.* **2002**, *74*, 1415.
6. Vankrunkelsven, S.; Clicq, D.; Pappaert, K.; Baron, G.V.; Desmet, G. *Anal. Chem.* **2004**, *76*, 3005.
7. Kuo, T.-C.; Sloan, L.A.; Sweedler, J.V.; Bohn, P.W. *Langmuir* **2001**, *17*, 6298.
8. Kuo, T.-C.; Cannon, Jr., D.M.; Shannon, M.A.; Bohn, P.W.; Sweedler, J.V. *Sens. Actuators A* **2003**, *102*, 223.
9. Kuo, T.-C.; Cannon, Jr., D.M.; Chen, Y.; Tulock, J.J.; Shannon, M.A.; Sweedler, J.V.; Bohn, P.W. *Anal. Chem.* **2003**, *75*, 1861.
10. Karlsson, R.; Karlsson, M.; Karlsson, A.; Cans, A.-S.; Bergenholtz, J.; Akerman, B.; Ewing, A.G.; Voinova, M.; Orwar, O. *Langmuir* **2002**, *18*, 4186.
11. Conlisk, A.T.; McFerran, J.; Zheng, Z.; Hansford, D. *Anal. Chem.* **2002**, *74*, 2139.
12. Burgence, D.; Nakache, F.R. *J. Phy. Chem.* **1964**, *68*, 1084.
13. McDonald, J.C.; Duffy, D.C.; Anderson, J.R.; Chiu, D.T.; Wu, H.; Schueller, O.J.A.; Whitesides, G.M. *Electrophoresis* **2000**, *21*, 27.
14. Guo, L.J.; Cheng, X.; Chou, C.-F. *Nano Letters* **2004**, *4*, 69.
15. Rice, C.L.; Whitehead, R. *J Phy. Chem.* **1965**, *69*, 4017.
16. Anderson, J.L.; Koh, W.-H. *J. Colloid Interf. Sci.* **1977**, 149–158.
17. Cintrón, J.M.; Colón, L.A. *Analyst* **2002**, *127*, 701.
18. Patel, K.D.; Jerkovich, A.D.; Link, J.C.; Jorgenson, J.W. *Anal. Chem.* **2004**, *76*, 5777.
19. Mellors, J.S.; Jorgenson, J.W. *Anal. Chem.* **2004**, *76*, 5441.
20. Chen, L.X.; Lee, S.; Choo, J.; Lee, E.K. *J. Micromech. Microeng.* **2008**, *18*, 013001, 22 pp.
21. Chen, L.X.; Ma, J.P.; Tan, F.; Guan, Y.F. *Sens. Actuators, B* **2003**, *88*, 260.
22. Chen, L.X.; Ma, J.P.; Guan, Y.F. *J. Chromatogr. A* **2004**, *1028*, 219.
23. Chen, L.X.; Guan, Y.F.; Ma, J.P.; Luo G.A.; Liu K.H. *J. Chromatogr. A* **2005**, *1064*, 19.
24. Chen, L.X.; Wang, H.L.; Ma, J.P.; Wang C.X.; Guan, Y.F. *Sens. Actuators, B* **2005**, *104*, 117.
25. Stöber, W.; Fink, A.; Bohn, E. *J. Colloid Interface Sci.* **1968**, *26*, 62.
26. Carlos, A.R.; Carlos A.P. *J. Phys. Chem. B.* **2003**, *107*, 4747.
27. Tsuda, T. *Anal. Chem.* **1987**, *59*, 521.
28. Boughtflower, B.J.; Uderwood, T.; Paterson, C.J. *Chromatographia* **1995**, *40*, 329.
29. Yan, C. Electrokinetic packing of capillary columns, United States Patent 5354163, 1995.
30. Knox, J.H.; Grant, I.H. *Chromatographia* **1987**, *24*, 135.
31. Knox, J.H. *Chromatographia* **1988**, *26*, 329.
32. Knox, J.H.; Grant, I.H. *Chromatographia* **1991**, *32*, 317.

Received January 22, 2008

Accepted February 22, 2008

Manuscript 6304